

# Impact of Embedded Endocannabinoids and Their Oxygenation by Lipoxygenase on Membrane Properties

Enrico Dainese,<sup>†,‡,||</sup> Annalaura Sabatucci,<sup>†,||</sup> Clotilde B. Angelucci,<sup>†</sup> Daniela Barsacchi,<sup>†</sup> Marco Chiarini,<sup>§</sup> and Mauro Maccarrone<sup>\*,†,‡</sup>

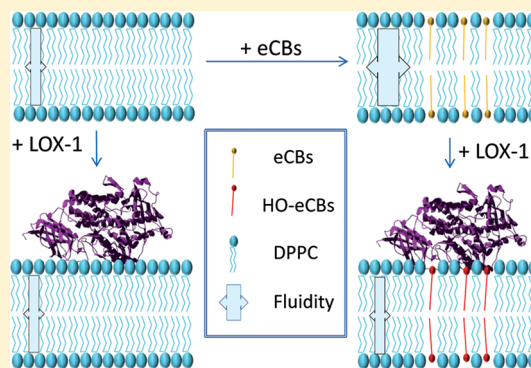
<sup>†</sup>Department of Biomedical Sciences, University of Teramo, Teramo, Italy

<sup>‡</sup>European Center for Brain Research (CERC)/Santa Lucia Foundation, Rome, Italy

<sup>§</sup>Department of Food Science, University of Teramo, Teramo, Italy

**ABSTRACT:** *N*-Arachidonylethanolamine (anandamide) and 2-arachidonoylglycerol are the best characterized endocannabinoids. Their biological activity is subjected to metabolic control whereby a dynamic equilibrium among biosynthetic, catabolic, and oxidative pathways drives their intracellular concentrations. In particular, lipoxygenases can generate hydroperoxy derivatives of endocannabinoids, endowed with distinct activities within cells. The *in vivo* interaction between lipoxygenases and endocannabinoids is likely to occur within cell membranes; thus, we sought to ascertain whether a prototypical enzyme like soybean (*Glycine max*) 15-lipoxygenase-1 is able to oxygenate endocannabinoids embedded in synthetic vesicles and how these substances could affect the binding ability of the enzyme to different lipid bilayers. We show that (i) embedded endocannabinoids increase membrane fluidity; (ii) 15-lipoxygenase-1 preferentially binds to endocannabinoid-containing bilayers; and that (iii) 15-lipoxygenase-1 oxidizes embedded endocannabinoids and thus reduces fluidity and local hydration of membrane lipids. Together, the present findings reveal further complexity in the regulation of endocannabinoid signaling within the central nervous system, disclosing novel control by oxidative pathways.

**KEYWORDS:** Endocannabinoids, FRET, FTIR, laurdan fluorescence, lipoxygenase activity, membrane binding



Endocannabinoids (eCBs) are derivatives of arachidonic acid (AA) and other poly unsaturated fatty acids that control basic biological processes, including cell choice between survival and death, immune response, energy homeostasis, and neurotransmission.<sup>1–4</sup> *N*-Arachidonylethanolamine (anandamide, AEA) and 2-arachidonoylglycerol (2-AG) are prototypical members of the two main groups of eCBs, the fatty acid amides and the monoacylglycerols, respectively.<sup>5,6</sup> Within the central nervous system (CNS), these substances have been largely recognized as major synaptic circuit breakers<sup>7</sup> and as regulators of neurotransmitter networks in neurodegenerative and neuroinflammatory diseases,<sup>8,9</sup> pain,<sup>10</sup> and brain trauma,<sup>11</sup> as well as cognitive and emotional behavior.<sup>12</sup>

An emerging topic in eCB research is the distribution of these compounds within cell membranes<sup>13</sup> and how interactions with the lipid environment might affect conformation<sup>14</sup> and signaling of eCBs.<sup>15</sup> In this context, a recent study has elucidated the arrangement of AEA in synthetic membranes made of 1,2-dipalmitoyl-*sn*-glycero-3-phosphocholine (DPPC) in the subgel phase.<sup>16</sup> It was shown that AEA adopts an extended conformation with its headgroup localized near the polar head region of the DPPC bilayer, and its methyl group near the center.<sup>16</sup> In addition, the presence of AEA at low concentrations (AEA/DPPC molar ratio, *R*, of 1:1000) did not produce perturbations to the lipid bilayer, whereas at higher

concentrations ( $1:100 < R < 1:10$ ) AEA did affect the chemico-physical and structural properties of the membrane.<sup>17</sup> The latter effect was likely a consequence of the formation of micro-environments, where AEA could also adopt nonextended conformations.<sup>17</sup>

Anandamide and 2-AG can be oxidized by lipoxygenases (linoleate/oxygen oxidoreductase, EC 1.13.11.12; LOXs),<sup>18,19</sup> a family of nonheme iron dioxygenases found in mammals and plants.<sup>20</sup> *In vitro*, hydroperoxy-anandamides (HO-AEAs) generated from AEA via LOX activity are powerful reversible inhibitors of fatty acid amide hydrolase (FAAH), the enzyme that terminates AEA signaling.<sup>21</sup> In addition, some HO-AEAs like 15-HO-AEA are able to activate *N*-acylphosphatidylethanolamine-specific phospholipase D *in vitro*.<sup>22</sup> The latter is the major biosynthetic enzyme for AEA.<sup>23</sup> Therefore, the possibility exists that HO-AEAs can act as natural modulators of eCBs metabolism *in vivo*,<sup>24</sup> an activity that might complement the

**Special Issue:** Therapeutic Potential of Endocannabinoid Metabolic Enzymes

**Received:** January 30, 2012

**Accepted:** February 24, 2012

**Published:** February 24, 2012



distinct effects of these compounds on different molecular targets within neuronal (and non-neuronal) cells.<sup>25,26</sup>

Soybean (*Glycine max* (L.) Merrill) 15-lipoxygenase-1 (LOX-1) has been widely used as a prototypical enzyme to study the functional and structural properties of the homologous family of LOXs.<sup>20</sup> Mammalian and plant LOXs comprise single polypeptide chains of ~75 kDa and ~90 kDa, respectively. The recently resolved crystal structure of a stable form of human 5-LOX<sup>27</sup> has confirmed that the overall topologies of mammalian and plant LOXs are very similar and characterized by a small N-terminal  $\beta$ -barrel domain (organized as a "polycystin-1, lipoxygenase, alpha-toxin" (PLAT) domain that marks the lipase/lipoxygenase superfamily) and a large catalytic C-terminal domain with the active site containing the iron cofactor.<sup>28</sup>

Many studies on the interaction of LOXs with membranes have been performed so far, mainly focusing on the structural effects of the lipids on protein conformation,<sup>29</sup> or on the role of the iron cofactor,<sup>30</sup> calcium,<sup>29–32</sup> or the N-terminal domain of LOXs<sup>33,34</sup> on their membrane binding ability. In-depth investigations performed by means of Fourier transformed infrared spectroscopy (FTIR), in both transmission and reflection modes, have shown that membrane binding and enzymatic activity of human 5-LOX increase with the degree of *cis*-unsaturation of the lipid acyl chain.<sup>35</sup> Conversely, possible effects of LOXs on membrane properties remain largely unknown. In this context, it should be recalled that different animal and plant lipoxygenases (soybean LOX-1 included) have been shown to oxygenate substrates that are embedded within lipid bilayers.<sup>36–38</sup>

Against this background, we sought to use laurdan generalized polarization (GP), FTIR, and fluorescence resonance energy transfer (FRET) on phospholipid liposomes, in order to (i) evaluate the structural effects of eCBs on the membranes; (ii) determine whether membrane-embedded eCBs are substrates of LOX-1; and (iii) characterize the membrane binding properties of LOX-1 within lipid bilayers containing embedded eCBs. Our findings show that the binding of an active LOX-1 to model membranes with embedded eCBs perturbs the chemico-physical properties of the membranes, by oxidizing the embedded substrates. In addition, the presence of embedded eCBs (in particular of AEA) was found to increase the membrane binding affinity of LOX-1, and HO-AEAs formed within the membrane by LOX-1 activity are suggested to play a role *in vivo* by modulating eCB tone through FAAH inhibition,<sup>39</sup> NAPE-PLD activation,<sup>22</sup> or by exerting distinct biological activities.<sup>25,26</sup>

## RESULTS AND DISCUSSION

**Modulation of Membrane Properties by Embedded eCBs and LOX-1 Protein.** First of all, we investigated the structural effects on DPPC model membranes of the two eCBs AEA and 2-AG. To this aim, laurdan GP spectra were obtained for 1 mM DPPC liposomes in the presence of 0.1 mM AEA, 2-AG, or AA (the latter substance used as a control). The application of the logistic formalism to these curves (see Methods) allowed us to calculate the melting parameters of the different liposomes, reported in Table 1. AEA, 2-AG, or AA within the membrane lowered the main transition temperature ( $T_m$ ) by ~2° and broadened the transition range (dT) to a similar extent (Figure 1A).

These results indicate that  $T_m$  values are mainly dependent on the acyl moiety of the lipid, which is the same for the three

**Table 1. Melting Parameters Obtained by Fitting the Laurdan GP Curves (see Methods) of DPPC Vesicles containing AEA, 2-AG or AA, in the Absence or Presence of 0.1  $\mu$ M LOX-1**

liposome	$T_m$	dT
DPPC	42.5 $\pm$ 0.2	-1.4 $\pm$ 0.2
DPPC/AEA	40.4 $\pm$ 0.3 <sup>a</sup>	-1.8 $\pm$ 0.3
DPPC/2-AG	40.5 $\pm$ 0.2 <sup>a</sup>	-2.4 $\pm$ 0.2
DPPC/AA	40.5 $\pm$ 0.2 <sup>a</sup>	-2.1 $\pm$ 0.2
DPPC/AEA+LOX-1	41.3 $\pm$ 0.2 <sup>b</sup>	-1.4 $\pm$ 0.2
DPPC/2-AG+LOX-1	41.2 $\pm$ 0.1 <sup>b</sup>	-2.2 $\pm$ 0.1
DPPC/AA+LOX-1	41.0 $\pm$ 0.1 <sup>b</sup>	-1.2 $\pm$ 0.1

<sup>a</sup> $p$  < 0.05 versus DPPC. <sup>b</sup> $p$  < 0.05 versus DPPC/corresponding lipid.

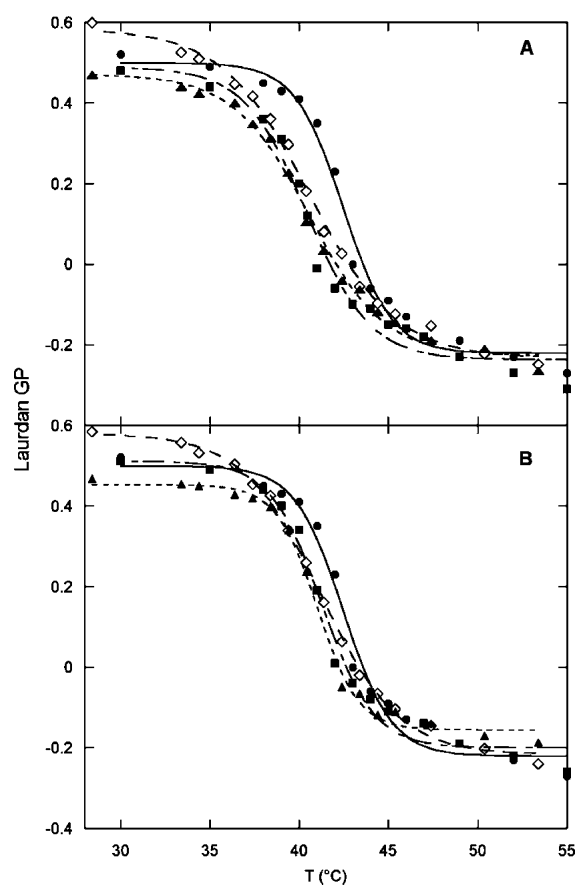


**Figure 1.** (A) Laurdan GP spectra of DPPC liposomes, in the absence (●) or presence of AEA (■), 2-AG (◇), or AA (▲) in a DPPC/compound 10:1 molar ratio. (B) GP spectra of the same samples as in panel A, after 20 min of incubation with 0.1  $\mu$ M LOX-1.

compounds. In line with these data, it has been already demonstrated that GP values are independent of the phospholipid headgroup<sup>40</sup> and that the physical interaction of different *N*-acylethanolamines (NAEs) with lipid membranes can modify the lipid  $T_m$  with a pattern dependent on the length of their acyl chain and on the number of double bonds.<sup>17,41</sup> Moreover, it has been shown that unsaturated NAEs slightly broaden the  $T_m$  range, an effect that might be related to the formation of lateral domains of the membrane with different lipid composition.<sup>41</sup>

Previous data have indicated that the interaction of LOXs with model membranes can induce an overall stabilization of both the protein and the membrane.<sup>28,29</sup> Here, to dissect the

effects of LOX-1 protein matrix from its enzyme activity on membrane properties, we used DPPC liposomes devoid of LOX-1 substrates, as well as AEA-containing LUVs incubated with the inactive apo-form of the enzyme. We found that in both cases, an enzyme concentration range of 0.1–1.0  $\mu\text{M}$  did not affect the  $T_m$  values of the membrane bilayer (data not shown). It has been demonstrated that the binding of LOX-1 to lipid membranes can be stabilized by  $\text{Ca}^{2+}$ <sup>31,42</sup> and that this ion is able to increase the amount of membrane-bound enzyme.<sup>30</sup> Therefore, we repeated our measurements after the addition of 100  $\mu\text{M}$   $\text{Ca}^{2+}$  and failed to detect any variation in the  $T_m$  of the DPPC liposomes (data not shown).

Once we ascertained that model membranes do not undergo structural modifications solely due to the interaction with the protein matrix, we further investigated the possible effect of the enzymatic activity of LOX-1 on  $T_m$  by using DPPC liposomes containing 0.1 mM AEA, 2-AG, or AA. After incubation with LOX-1, the laurdan GP curves of three model membranes of different compositions converged toward that obtained with pure DPPC (Figure 1B and Table 1). In all cases,  $T_m$  values raised by  $\sim 0.6$   $^\circ\text{C}$ , and the transition range showed a sharper slope (less markedly in the case of 2-AG), which is indicative of a more homogeneous lipid environment.<sup>43</sup> These data suggest that eCBs and AA embedded within the membrane can be oxygenated by LOX-1, thus leading to a decrease of membrane fluidity. Interestingly, LOX-1 seemed to have a larger impact on the chemico-physical properties of the bilayer with embedded AEA, as demonstrated by the dT value of AEA LUVs that tended to that of pure DPPC after LOX-1 treatment.

**Enzymatic Activity of LOX-1 on Free and Embedded eCBs.** It has been already demonstrated that free eCBs can be substrates of LOXs,<sup>39,44,45</sup> but experimental evidence that membrane-embedded eCBs can also be oxygenated by LOX-1 is still lacking. To ascertain whether the observed chemico-physical modifications of membrane lipids could be attributed to enzymatic oxygenation of embedded eCBs by LOX-1, we analyzed the kinetic parameters of LOX-1 using free AEA and 2-AG, and compared them to those obtained with the canonical substrate AA.  $K_m$  values in Table 2 show that LOX-1 has a

**Table 2. Kinetic Parameters of Soybean LOX-1 with Different Substrates in Solution**

	AA	AEA	2-AG
$K_m$ ( $\mu\text{M}$ )	$16.1 \pm 3.0$	$24.0 \pm 3.0$	$45.6 \pm 4.0$
$V_{\text{max}}$ ( $\text{nmol s}^{-1} \text{mg}^{-1}$ )	$89.9 \pm 5.0$	$6.4 \pm 0.3$	$4.2 \pm 0.2$
$K_{\text{cat}}$	$27.2 \pm 1.5$	$1.9 \pm 0.1$	$1.3 \pm 0.1$
$K_{\text{cat}}/K_m$	$1.7 \pm 0.4$	$0.10 \pm 0.01$	$0.030 \pm 0.004$

higher affinity toward AA, followed by AEA ( $\sim 1.5$ -fold lower) and 2-AG ( $\sim 3$ -fold lower). Then, we analyzed the catalytic activity of LOX-1 using membrane-embedded AEA at different enzyme concentrations, showing that hydroperoxy derivatives of AEA can be formed in a concentration-dependent manner also when AEA is embedded within a membrane bilayer (Figure 2).

Taken together, these results indicate that LOX-1 oxygenates membrane-embedded eCBs (as well as AA), thus reducing membrane fluidity in a manner that parallels the enzyme affinity toward its substrates. These novel findings add a new dimension to the oxidative mechanisms that regulate the intracellular concentration of eCBs.<sup>46</sup>

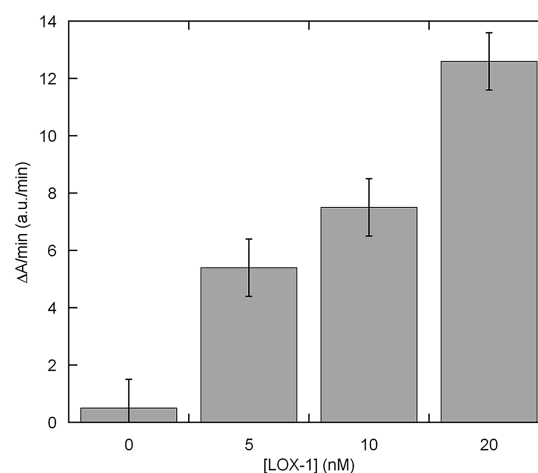


**Figure 2.** Formation of hydroperoxy derivatives from membrane-embedded AEA at different LOX-1 concentrations.

### Membrane Binding of LOX-1 to eCB-Containing Bilayers.

Keeping in mind that the eCBs derive from membrane lipids and that their endogenous tone is modulated by oxidative enzymes,<sup>46</sup> understanding the membrane binding properties of the latter enzymes could help to further clarify the regulation of the biological activity of these lipids. Thus, we analyzed the membrane binding properties of LOX-1 to eCB-containing membranes by analyzing FRET between the Trp fluorophores of the protein and the Pyrene-PE acceptor embedded within the membrane. The increase of Trp quenching was analyzed as a function of lipid concentration, in the absence or presence of calcium ions in solution, corroborating the evidence that LOX-1 interaction with membranes is strengthened by this divalent cation.<sup>30</sup> FRET curves clearly showed a hyperbolic shape (Figure 3) and could be fitted according to a standard binding curve with a half-saturation binding constant ( $[L]_{1/2}$ ) of  $39.2 \pm 3.7$   $\mu\text{M}$  for pure DPPC membranes (Table 3).

Remarkably, both in the case of DPPC/AEA and DPPC/2-AG membranes (DPPC/eCB molar ratio of 10:1), lower values

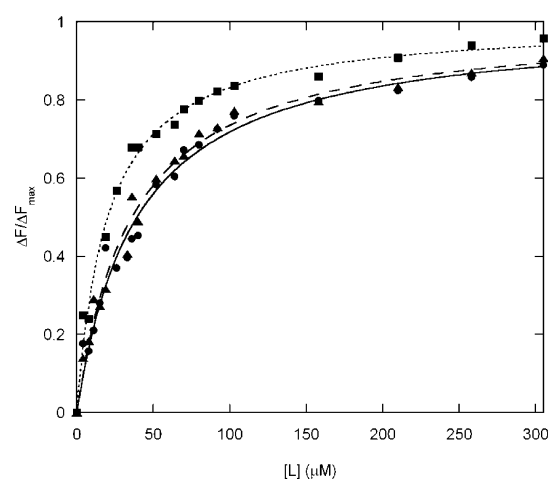


**Figure 3.** FRET analysis of LOX-1 binding to different LUV membranes. Hyperbolic fitting of the quenching of Trp fluorescence upon enzyme binding, as a function of liposome concentration. ●, DPPC liposomes; ■, DPPC/AEA (10:1 molar ratio) liposomes; ▲, DPPC/AA (10:1 molar ratio) liposomes. The values of lipid concentrations at half saturation are reported in Table 3.

**Table 3. Comparison of Membrane Binding Affinity of LOX-1 toward Different Lipid Bilayers**

liposome	$[L]_{1/2}$ ( $\mu\text{M}$ )
DPPC	$39.2 \pm 3.7$
DPPC/AEA	$20.2 \pm 1.6^a$
DPPC/2-AG	$19.0 \pm 1.0^a$
DPPC/AA	$35.9 \pm 2.9$

<sup>a</sup> $p < 0.05$  versus DPPC.

of  $[L]_{1/2}$  were obtained (Table 3), indicating that the protein–membrane interaction was almost doubled in the presence of each eCB. No preferential binding of LOX-1 was observed in the presence of embedded AA (Table 3), nor upon addition of ethanolamine or glycerol (that are eCBs moieties) on DPPC liposomes (data not shown).

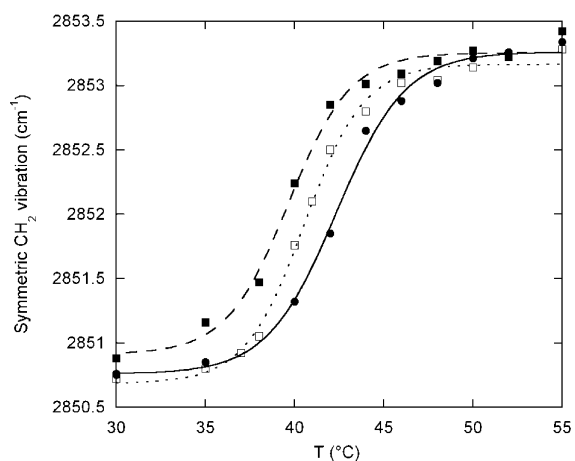
**Analysis of Membrane Fluidity and Hydration by FTIR.** LOX-1 preferred AEA better than 2-AG as a substrate (Table 2); thus, we further investigated the enzyme-induced membrane modifications by transmission FTIR under the same experimental conditions used for laurdan GP assays. In order to calculate  $T_m$  values of liposomes, the frequency of the  $\text{CH}_2$  symmetric vibrational band was analyzed. The  $T_m$  values, calculated by applying eq 2 to the FTIR spectra and reported in Table 4, were in good accordance with the laurdan GP results.

**Table 4. Analysis of the  $\text{CH}_2$  Symmetric Vibrational Band Frequencies of DPPC/AEA Liposomes, in the Absence or Presence of LOX-1**

liposome	$T_m$	$A_1$ ( $\text{cm}^{-1}$ )	$A_2$ ( $\text{cm}^{-1}$ )	dT
DPPC	$42.3 \pm 0.2$	$2850.8 \pm 0.1$	$2853.3 \pm 0.1$	$1.9 \pm 0.2$
DPPC/AEA	$39.6 \pm 0.3^a$	$2850.9 \pm 0.1$	$2853.2 \pm 0.1$	$1.7 \pm 0.3$
DPPC/AEA + LOX-1	$40.5 \pm 0.2^{a,b}$	$2850.7 \pm 0.1$	$2853.2 \pm 0.1$	$1.2 \pm 0.1$

<sup>a</sup> $p < 0.05$  versus DPPC. <sup>b</sup> $p < 0.05$  versus DPPC/AEA.

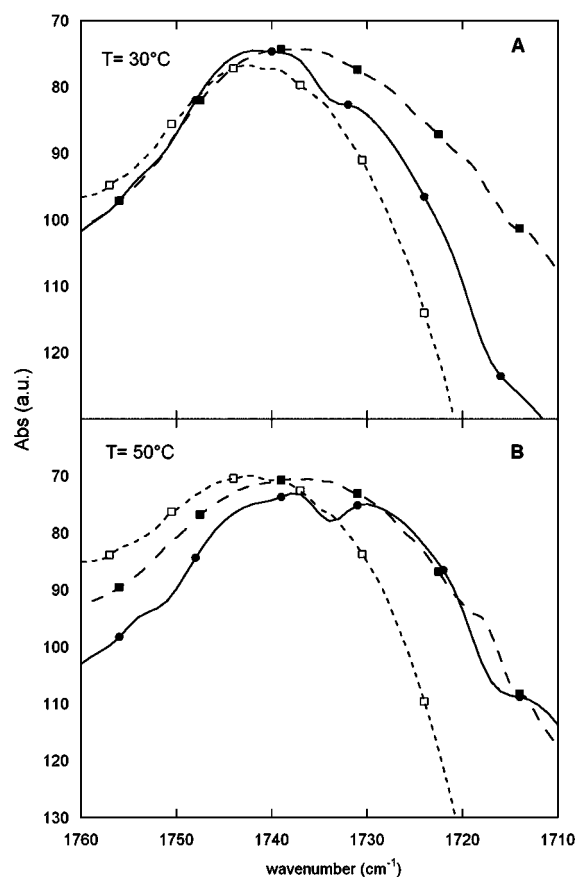
As already seen in laurdan fluorescence, the analysis of the thermal profiles of the  $\text{CH}_2$  vibrational band showed that the presence of AEA affects the structural properties of DPPC liposomes, lowering the  $T_m$  by  $2.7 \pm 0.5$  °C (Figure 4 and Table 4).

**Figure 4.** Thermal profile of the symmetric  $\text{CH}_2$  vibrational band of DPPC/AEA liposomes, before and after incubation with  $0.1 \mu\text{M}$  LOX-1. ●, pure DPPC; ■, DPPC in the presence of AEA (10:1 molar ratio); □, DPPC/AEA liposomes after incubation with  $0.1 \mu\text{M}$  LOX-1.

In addition, FTIR analysis allowed us to demonstrate a higher vibrational frequency of the methylene group in the presence of AEA, both in the gel and in the liquid crystalline phase (Table 1), indicating that AEA has a fluidizing effect on the membrane. After incubation with LOX-1,  $T_m$  was raised leading to a value similar to that of pure DPPC, again extending the results obtained with laurdan fluorescence. Additionally, the vibrational frequency was lowered, indicating a higher rigidity of the membrane.

FTIR analysis allowed us also to measure the hydration of the membrane bilayer at the water/lipid interface and possible modifications due to LOX-1. Thus, we analyzed the  $\text{C}=\text{O}$  vibrational band of the ester carbonyl group at the polar/apolar interface of phospholipids. This band can be split into two components, centered near  $1740$  and  $1728 \text{ cm}^{-1}$ , which arise from populations of “free” and “hydrogen-bonded” ester carbonyl groups, respectively (see ref 47 and references therein). In pure DPPC SUVs upon phase transition, an increase of the relative contribution of the lower frequency band was observed, reflecting an increase of hydration at the phospholipid hydrophobic–hydrophilic interface (Figure 5).

In the presence of AEA, the band was broader, probably because of an overall higher hydration of membrane lipids. Interestingly, upon incubation of AEA-containing membranes

**Figure 5.**  $\text{CO}$  vibrational band of pure DPPC liposomes (●) was broader in the presence of 10% mol AEA (■). Incubation of DPPC/AEA liposomes (10:1 molar ratio) with  $0.1 \mu\text{M}$  LOX-1 (□) led to a narrower band, which was shifted to higher wavenumbers both in the gel (upper panel,  $T = 30$  °C) and in the liquid crystalline phase (lower panel,  $T = 50$  °C). This finding is suggestive of phospholipid dehydration upon interaction with LOX-1.

with LOX-1, the component at lower frequency disappeared (both below and above the  $T_m$  value) and a unique, narrower peak centered at  $\sim 1740\text{ cm}^{-1}$  appeared; this finding is indicative of a dehydration process of the DPPC/AEA bilayer upon protein binding. Taken together, these data clearly indicate that both in the gel and in the liquid crystalline phase the interaction of LOX-1 with AEA-containing membranes leads to a dehydration of the lipid bilayer. This is reminiscent of the known activation mechanism of enzymes (like phospholipases), that work at the membrane/water interface, where water molecules are excluded from the active site.<sup>48</sup>

## CONCLUDING REMARKS

Altogether, the present data demonstrate that eCBs within lipid bilayers composed of fully saturated acyl chains can have a fluidizing effect, as documented by the lower transition temperature and the higher vibrational frequency of the methylene group in DPPC/AEA SUVs, in both the gel and the liquid crystalline phase. Additionally, our results demonstrate that LOX-1 is active on membrane-embedded eCBs, in particular on those containing AEA. In fact, both laurdan GP and FTIR  $\text{CH}_2$  vibrational band of DPPC/AEA liposomes after incubation with LOX-1 tended to superimpose on those of pure DPPC, probably due to a more ordered packing of the AEA acyl chain upon oxygenation by LOX-1. In line with these data, it has been already reported that the main effect of peroxidation on lipid dynamics and membrane order is a general decrease of the membrane fluidity.<sup>49,50</sup> Moreover, here we demonstrate that membrane affinity of LOX-1 in the presence of calcium ions is almost doubled when membranes contain AEA or 2-AG. This observation suggests a preferential interaction of LOX-1 with eCBs-containing membranes, that *in vivo* could contribute to the different subcellular localization of the enzyme.<sup>51,52</sup> Furthermore, here we demonstrate that upon LOX-1 binding, AEA-containing liposomes undergo a partial dehydration of the membrane surface, as documented by the spectral shift of the carbonyl stretching band in FTIR analysis. This finding is in line with previous data on the interaction of human 5-LOX with synthetic vesicles<sup>29</sup> and provides further insights into the role of the surface properties of a lipid bilayer on membrane-interacting enzymes, like phospholipases, that undergo interfacial activation by the surrounding lipids.<sup>48</sup>

The present data also suggest that HO-AEAs can be generated by LOX-1-dependent oxygenation of membrane-embedded AEA and could diffuse laterally within the lipid bilayer to inhibit FAAH,<sup>39</sup> and/or activate NAPE-PLD,<sup>22</sup> thus sustaining a hyper-tone of AEA and subsequently an enhancement of its signaling. In addition, the observation that eCBs can increase membrane fluidity, whereas their oxygenation by LOX-1 can reduce it, suggests that the eCBs/LOX-1 couple might regulate indirectly those receptors that are sensitive to the membrane environment.<sup>15</sup> In this context, interaction with the surrounding lipids may serve as a mechanochemical mediator of type-1 cannabinoid receptor signaling, with implications also for the efficacy of small molecule therapeutics.<sup>53</sup> Therefore, the effect of eCBs and their oxygenation on membrane properties seems to add further complexity to the already intricate networks at the basis of eCB signaling.

## METHODS

**Materials and Enzymes.** All chemicals were of the purest analytical grade. DPPC, AEA, 2-AG, AA, and Laurdan were from Sigma Chemical Co. (St. Luis, MO, USA). Pyrene-PE was from Avanti

Polar Lipids, Inc. (Alabaster, AL, USA). 15-Lipoxygenase-1 was purified from soybean (*Glycine max* (L.) Merrill, Williams) seeds, as described.<sup>28</sup> The inactive apo-form of the enzyme was obtained upon metal removal by chelating agents, as previously reported.<sup>30</sup>

**Preparation of Liposomes.** DPPC large unilamellar vesicles (LUVs) were prepared at a final concentration of 1 mM, in the absence or presence of 0.1 mM AEA, 2-AG, or AA (lipid/DPPC molar ratio of 1:10), by standard hydration and extrusion methods in 50 mM Tris/HCl buffer, pH 7.6.<sup>30</sup> For the measurements in the presence of calcium ions, 0.1 mM EGTA and 0.3 mM  $\text{CaCl}_2$  were added to the buffer. Small unilamellar vesicles (SUVs) for FTIR measurements were prepared by the same procedure in the same buffer at a final concentration of 55 mM, in the absence or presence of 5 mM AEA (lipid/DPPC molar ratio of 1:10). In order to obtain SUVs, samples were sonicated at  $T > T_m$  with a tip sonicator (Bandelin electronic, Berlin, Germany), until the cloudy suspension became clear.<sup>54</sup>

**Fluorescence Measurements.** Fluorescence measurements were performed in a Perkin-Elmer LSBS50 fluorimeter (PerkinElmer, Waltham, MA, USA), using a  $10 \times 2$  mm path length quartz fluorescence microcuvette. The temperature in the sample holder was kept constant by an external bath circulator and was carefully checked by a thermocouple. For generalized polarization (GP) measurements, the laurdan probe was added to 1 mM LUVs at a final concentration of 1  $\mu\text{M}$  (probelipid molar ratio of 1:10<sup>3</sup>). LOX-1 was added to the liposome solutions at a final protein concentration of 0.1  $\mu\text{M}$  (protein/liposomes molar ratio of 1:10<sup>4</sup>) and was incubated at 30 °C for 20 min before fluorescence measurements. Laurdan emission spectra were recorded in triplicate in a 300–600 nm range, using an excitation wavelength of 340 nm. Laurdan GP was calculated according to the following formula, as reported.<sup>40,55</sup>

$$\text{GP} = (I_b - I_r)/(I_b + I_r) \quad (1)$$

where  $I_b$  is the laurdan fluorescence emission intensity at  $\lambda = 440$  nm;  $I_r$  is the intensity at 490 nm. The fluorescence spectra of liposomes without laurdan were used as the background signal (minor differences in the total lipid concentrations were corrected by normalizing the sample and background curves at the wavelength of 600 nm, where the laurdan signal is negligible).

**FRET Measurements.** Membrane insertion of LOX-1 was monitored by FRET experiments, where protein tryptophans served as donors and the Pyrene PE fluorescent probe, incorporated into 1 mM LUVs at a concentration of 10 nM (probe/lipid molar ratio of 1:10<sup>5</sup>), as a fluorescence acceptor.<sup>35</sup> Fluorescence emission spectra were recorded in the wavelength range from 300 to 600 nm, using an excitation wavelength of 295 nm. The binding isotherms were built as already reported.<sup>30</sup>

**FTIR Measurements.** FTIR measurements were performed using a Perkin-Elmer Spectrum ONE (Perkin-Elmer, Waltham, MA, USA) FTIR spectrometer, with a demountable temperature-controlled transmission cell for liquid samples (Specac Ltd. Buckingham, Slough, UK) and equipped with two  $\text{CaF}_2$  windows. The path length chosen was 0.05 mm, giving a total volume of  $\sim 20\ \mu\text{L}$ . The temperature control was achieved by a circulating water bath. The wavenumber scan range was from 3600 to 900  $\text{cm}^{-1}$ , with a resolution of 2  $\text{cm}^{-1}$ . LOX-1 solutions were added to liposomes to a final protein concentration of 1  $\mu\text{M}$  (protein/liposomes molar ratio of 1:5  $\times 10^4$ ) and were incubated at 30 °C for 60 min before measurements. For each spectrum, 16 scans were collected and averaged.

**Laurdan GP and FTIR Data Analysis.** As the GP of the Laurdan probe accounts for the variations of polarity of the solvent mainly arising in the region of the acyl chains of the phospholipids,<sup>40</sup> and the  $\text{CH}_2$  stretching mode accounts for the variations of the vibrational modes in the same region of the phospholipids when a phase transition takes place, we applied a logistic equation to fit both GP and FTIR curves, as described.<sup>40,55</sup>

The applied sigmoidal function was the following:

$$y = \frac{A_1 - A_2}{1 + e^{-T - T_m/dT}} + A_2 \quad (2)$$

In the case of laurdan GP, the parameters  $A_1$  and  $A_2$  are the asymptotic values of GP at the lowest and highest temperature, respectively. Instead, for FTIR spectra  $A_1$  and  $A_2$  are the  $\text{CH}_2$  symmetric stretching band frequencies for the solid-like gel phase ( $\beta$ -phase) and the liquid disordered crystalline phase ( $\alpha$ -phase), respectively.  $dT$  is a measure of the rate of change, while  $T_m$  is the main transition temperature of lipids.

**Enzyme Assays.** LOX-1 activity was assayed using a DU 640 spectrophotometer equipped with a Peltier temperature control system (Beckman Instruments, Brea, CA, USA). All measurements were performed at 25 °C. Reagents were dissolved in 50 mM Tris/HCl buffer (pH 7.6), containing 0.1 mM EGTA and 0.3 mM  $\text{CaCl}_2$ . Enzymatic activity was evaluated by monitoring the formation of conjugated diene products of arachidonic acid, AEA or 2-AG at 234 nm ( $\epsilon = 25000 \text{ M}^{-1}\text{cm}^{-1}$ ), using a LOX-1 concentration of 7 nM and a substrate concentration range from 5  $\mu\text{M}$  to 60  $\mu\text{M}$ .<sup>34</sup> The formation of conjugated dienes from embedded AEA was followed in 0.1 mM DPPC LUVs containing 10  $\mu\text{M}$  AEA at three different enzyme concentrations (5 nM, 10 nM, and 20 nM). Kinetic parameters of the reaction catalyzed by LOX-1, i.e., apparent Michaelis–Menten constant ( $K_M$ ), maximum velocity ( $V_{\text{max}}$ ), catalytic constant ( $K_{\text{cat}}$ ), and catalytic efficiency ( $K_{\text{cat}}/K_M$ ), were determined as previously described.<sup>30</sup>

**Statistical Analysis.** Data reported in this article are the means ( $\pm$ SD) of at least three independent determinations, each performed in triplicate. Data analysis was performed by nonlinear regression with the Kaleidagraph 4.0 program (Synergy Software, Reading, PA, USA). Statistical analysis of kinetic data was performed by the nonparametric Mann–Whitney U test, analyzing experimental data by means of the Prism 5 program (GraphPAD Software for Science, San Diego, CA, USA).

## AUTHOR INFORMATION

### Corresponding Author

\*Department of Biomedical Sciences, University of Teramo, Piazza A. Moro 45, 64100 Teramo, Italy. Tel: 39-0861-266875. Fax: 39-0861-266877. E-mail: mmaccarrone@unite.it.

### Author Contributions

<sup>†</sup>These authors contributed equally to the study.

### Funding

This work was supported by Ministero dell'Istruzione, dell'Università e della Ricerca (Grant PRIN 2008), and by Fondazione della Cassa di Risparmio di Teramo TERCAS (Contract 2009-2012) to MM.

### Notes

The authors declare no competing financial interest.

## ABBREVIATIONS

AA, arachidonic acid; AEA, *N*-arachidonylethanolamine; 2-AG, 2-arachidonoylglycerol; CNS, central nervous system; Dansyl-DHPE, *N*-(5-dimethylaminonaphthalene-1-sulfonyl)-1,2-dihexadecanoyl-*sn*-glycero-3-phosphoethanolamine; DPPC, 1,2-dipalmitoyl-*sn*-glycero-3-phosphocholine; eCB, endocannabinoid; FAAH, fatty acid amide hydrolase; FRET, fluorescence resonance energy transfer; FTIR, Fourier transformed infrared spectroscopy; GP, generalized polarization; HO-AEA, hydroperoxy-anandamide; HO-eCBs, hydroperoxy-endocannabinoids; Laurdan, 2-dimethylamino-(6-lauroyl)-naphthalene; LOX-1, 15-lipoxygenase-1; LUV, large unilamellar vesicle; NAE, *N*-acylethanolamine; NAPE-PLD, *N*-acylphosphatidylethanolamine-specific phospholipase D; PC, phosphatidylcholine; PLAT, polycystin-1, lipoxygenase, alpha-toxin; Pyrene PE, 1,2-dioleoyl-*sn*-glycero-3-phosphoethanolamine-*N*-(1-pyrenesulfonyl); SUV, small unilamellar vesicle

## REFERENCES

- (1) Ligresti, A., Cascio, M. G., and Di Marzo, V. (2005) Endocannabinoid metabolic pathways and enzymes. *CNS Neurol. Disord.: Drug Targets* 4, 615–623.
- (2) Kogan, N. M., and Mechoulam, R. (2006) The chemistry of endocannabinoids. *J. Endocrinol. Invest* 29, 3–14.
- (3) Basavarajappa, B. S. (2007) Critical enzymes involved in endocannabinoid metabolism. *Protein Pept. Lett.* 14, 237–246.
- (4) Maccarrone, M., and Finazzi-Agrò, A. (2002) Endocannabinoids and their actions. *Vitam. Horm.* 65, 225–255.
- (5) Pop, E. (1999) Cannabinoids, endogenous ligands and synthetic analogs. *Curr. Opin. Chem. Biol.* 3, 418–425.
- (6) Di Marzo, V. (2008) Endocannabinoids: synthesis and degradation. *Rev. Physiol Biochem. Pharmacol.* 160, 1–24.
- (7) Katona, L., and Freund, T. F. (2008) Endocannabinoid signaling as a synaptic circuit breaker in neurological disease. *Nat. Med.* 14, 923–930.
- (8) Wolf, S. A., Tauber, S., and Ullrich, O. (2008) CNS immune surveillance and neuroinflammation: endocannabinoids keep control. *Curr. Pharm. Des.* 14, 2266–2278.
- (9) Centonze, D., Finazzi-Agrò, A., Bernardi, G., and Maccarrone, M. (2007) The endocannabinoid system in targeting inflammatory neurodegenerative diseases. *Trends Pharmacol. Sci.* 28, 180–187.
- (10) Guindon, J., and Hohmann, A. G. (2009) The endocannabinoid system and pain. *CNS Neurol. Disord.: Drug Targets* 8, 403–421.
- (11) Shohami, E., Cohen-Yeshurun, A., Magid, L., Algali, M., and Mechoulam, R. (2011) Endocannabinoids and traumatic brain injury. *Br. J. Pharmacol.* 163, 1402–1410.
- (12) Zanettini, C., Panlilio, L. V., Alicki, M., Goldberg, S. R., Haller, J., and Yasar, S. (2011) Effects of endocannabinoid system modulation on cognitive and emotional behavior. *Front. Behav. Neurosci.* 5, 57.
- (13) Rimmerman, N., Hughes, H. V., Bradshaw, H. B., Pazos, M. X., Mackie, K., Prieto, A. L., and Walker, J. M. (2008) Compartmentalization of endocannabinoids into lipid rafts in a dorsal root ganglion cell line. *Br. J. Pharmacol.* 153, 380–389.
- (14) Barnett-Norris, J., Lynch, D., and Reggio, P. H. (2005) Lipids, lipid rafts and caveolae: their importance for GPCR signaling and their centrality to the endocannabinoid system. *Life Sci.* 77, 1625–1639.
- (15) Maccarrone, M., Bernardi, G., Finazzi-Agrò, A., and Centonze, D. (2011) Cannabinoid receptor signalling in neurodegenerative diseases: a potential role for membrane fluidity disturbance. *Br. J. Pharmacol.* 163, 1379–1390.
- (16) Tian, X., Guo, J., Yao, F., Yang, D. P., and Makriyannis, A. (2005) The conformation, location, and dynamic properties of the endocannabinoid ligand anandamide in a membrane bilayer. *J. Biol. Chem.* 280, 29788–29795.
- (17) Ambrosi, S., Ragni, L., Ambrosini, A., Paccamiccio, L., Mariani, P., Fiorini, R., Bertoli, E., and Zolese, G. (2005) On the importance of anandamide structural features for its interactions with DPPC bilayers: effects on PLA2 activity. *J. Lipid Res.* 46, 1953–1961.
- (18) Hampson, A. J., Hill, W. A., Zan-Phillips, M., Makriyannis, A., Leung, E., Eglen, R. M., and Bornheim, L. M. (1995) Anandamide hydroxylation by brain lipoxygenase: metabolite structures and potencies at the cannabinoid receptor. *Biochim. Biophys. Acta* 1259, 173–179.
- (19) Ueda, N., Yamamoto, K., Yamamoto, S., Tokunaga, T., Shirakawa, E., Shinkai, H., Ogawa, M., Sato, T., Kudo, I., Inoue, K., Takizawa, H., Nagano, T., Hirobe, M., Matsuki, N., and Saito, H. (1995) Lipoxygenase-catalyzed oxygenation of arachidonylethanolamide, a cannabinoid receptor agonist. *Biochim. Biophys. Acta* 1254, 127–134.
- (20) Brash, A. R. (1999) Lipoxygenases: occurrence, functions, catalysis, and acquisition of substrate. *J. Biol. Chem.* 274, 23679–23682.
- (21) van der Stelt, M., Veldhuis, W. B., Maccarrone, M., Bar, P. R., Nicolay, K., Veldink, G. A., Di, M., V., and Vliegthart, J. F. (2002) Acute neuronal injury, excitotoxicity, and the endocannabinoid system. *Mol. Neurobiol.* 26, 317–346.

- (22) Amadio, D., Fezza, F., Catanzaro, G., Incani, O., van Zadelhoff, G., Finazzi-Agrò, A., and Maccarrone, M. (2010) Methylation and acetylation of 15-hydroxyanandamide modulate its interaction with the endocannabinoid system. *Biochimie* 92, 378–387.
- (23) Ueda, N., Tsuboi, K., and Uyama, T. (2010) Enzymological studies on the biosynthesis of N-acylethanolamines. *Biochim. Biophys. Acta* 1801, 1274–1285.
- (24) Maccarrone, M. (2004) Inhibition of anandamide hydrolysis: cells also know how to do it. *Trends Mol. Med.* 10, 13–14.
- (25) Veldhuis, W. B., van der Stelt, M., Wadman, M. W., van Zadelhoff, G., Maccarrone, M., Fezza, F., Veldink, G. A., Vliegthart, J. F., Bar, P. R., Nicolay, K., and Di Marzo, V. (2003) Neuroprotection by the endogenous cannabinoid anandamide and arvanil against in vivo excitotoxicity in the rat: role of vanilloid receptors and lipoxygenases. *J. Neurosci.* 23, 4127–4133.
- (26) Rouzer, C. A., and Marnett, L. J. (2008) Non-redundant functions of cyclooxygenases: oxygenation of endocannabinoids. *J. Biol. Chem.* 283, 8065–8069.
- (27) Gilbert, N. C., Bartlett, S. G., Waight, M. T., Neau, D. B., Boeglin, W. E., Brash, A. R., and Newcomer, M. E. (2011) The structure of human 5-lipoxygenase. *Science* 331, 217–219.
- (28) Mei, G., Di Venere, A., Nicolai, E., Angelucci, C. B., Ivanov, I., Sabatucci, A., Dainese, E., Kuhn, H., and Maccarrone, M. (2008) Structural properties of plant and mammalian lipoxygenases. Temperature-dependent conformational alterations and membrane binding ability. *Biochemistry* 47, 9234–9242.
- (29) Pande, A. H., Moe, D., Nemeč, K. N., Qin, S., Tan, S., and Tatulian, S. A. (2004) Modulation of human 5-lipoxygenase activity by membrane lipids. *Biochemistry* 43, 14653–14666.
- (30) Dainese, E., Angelucci, C. B., Sabatucci, A., De, F., V, Mei, G., and Maccarrone, M. (2010) A novel role for iron in modulating the activity and membrane-binding ability of a trimmed soybean lipoxygenase-1. *FASEB J.* 24, 1725–1736.
- (31) Tatulian, S. A., Steczko, J., and Minor, W. (1998) Uncovering a calcium-regulated membrane-binding mechanism for soybean lipoxygenase-1. *Biochemistry* 37, 15481–15490.
- (32) Oldham, M. L., Brash, A. R., and Newcomer, M. E. (2005) Insights from the X-ray crystal structure of coral 8R-lipoxygenase: calcium activation via a C2-like domain and a structural basis of product chirality. *J. Biol. Chem.* 280, 39545–39552.
- (33) Aleem, A. M., Jankun, J., Dignam, J. D., Walther, M., Kuhn, H., Svergun, D. I., and Skrzypczak-Jankun, E. (2008) Human platelet 12-lipoxygenase, new findings about its activity, membrane binding and low-resolution structure. *J. Mol. Biol.* 376, 193–209.
- (34) Maccarrone, M., Salucci, M. L., van Zadelhoff, G., Malatesta, F., Veldink, G., Vliegthart, J. F., and Finazzi-Agrò, A. (2001) Tryptic digestion of soybean lipoxygenase-1 generates a 60 kDa fragment with improved activity and membrane binding ability. *Biochemistry* 40, 6819–6827.
- (35) Pande, A. H., Qin, S., and Tatulian, S. A. (2005) Membrane fluidity is a key modulator of membrane binding, insertion, and activity of 5-lipoxygenase. *Biophys. J.* 88, 4084–4094.
- (36) Kuhn, H., Belkner, J., Wiesner, R., and Brash, A. R. (1990) Oxygenation of biological membranes by the pure reticulocyte lipoxygenase. *J. Biol. Chem.* 265, 18351–18361.
- (37) Maccarrone, M., van Aarle, P. G., Veldink, G. A., and Vliegthart, J. F. (1994) In vitro oxygenation of soybean biomembranes by lipoxygenase-2. *Biochim. Biophys. Acta* 1190, 164–169.
- (38) Kato, M., Nishiyama, J., and Kuninori, T. (1998) Reactivity of soybean lipoxygenase-1 to linoleic acid entrapped in phosphatidylcholine vesicles. *J. Biochem. (Tokyo)* 124, 294–299.
- (39) van der Stelt, M., van Kuik, J. A., Bari, M., van Zadelhoff, G., Leeftang, B. R., Veldink, G. A., Finazzi-Agrò, A., Vliegthart, J. F., and Maccarrone, M. (2002) Oxygenated metabolites of anandamide and 2-arachidonoylglycerol: conformational analysis and interaction with cannabinoid receptors, membrane transporter, and fatty acid amide hydrolase. *J. Med. Chem.* 45, 3709–3720.
- (40) Parasassi, T., De Stasio, G., Ravagnan, G., Rusch, R. M., and Gratton, E. (1991) Quantitation of lipid phases in phospholipid vesicles by the generalized polarization of Laurdan fluorescence. *Biophys. J.* 60, 179–189.
- (41) Zolse, G., Wozniak, M., Mariani, P., Saturni, L., Bertoli, E., and Ambrosini, A. (2003) Different modulation of phospholipase A2 activity by saturated and monounsaturated N-acylethanolamines. *J. Lipid Res.* 44, 742–753.
- (42) Walther, M., Wiesner, R., and Kuhn, H. (2004) Investigations into calcium-dependent membrane association of 15-lipoxygenase-1. Mechanistic roles of surface-exposed hydrophobic amino acids and calcium. *J. Biol. Chem.* 279, 3717–3725.
- (43) Parasassi, T., Loiero, M., Raimondi, M., Ravagnan, G., and Gratton, E. (1993) Absence of lipid gel-phase domains in seven mammalian cell lines and in four primary cell types. *Biochim. Biophys. Acta* 1153, 143–154.
- (44) Edgemond, W. S., Hillard, C. J., Falck, J. R., Kearns, C. S., and Campbell, W. B. (1998) Human platelets and polymorphonuclear leukocytes synthesize oxygenated derivatives of arachidonylethanolamide (anandamide): their affinities for cannabinoid receptors and pathways of inactivation. *Mol. Pharmacol.* 54, 180–188.
- (45) Kozak, K. R., Gupta, R. A., Moody, J. S., Ji, C., Boeglin, W. E., DuBois, R. N., Brash, A. R., and Marnett, L. J. (2002) 15-Lipoxygenase metabolism of 2-arachidonoylglycerol. Generation of a peroxisome proliferator-activated receptor alpha agonist. *J. Biol. Chem.* 277, 23278–23286.
- (46) Maccarrone, M., Dainese, E., and Oddi, S. (2010) Intracellular trafficking of anandamide: new concepts for signaling. *Trends Biochem. Sci.* 35, 601–608.
- (47) Mannock, D. A., Lewis, R. N., and McElhaney, R. N. (2006) Comparative calorimetric and spectroscopic studies of the effects of lanosterol and cholesterol on the thermotropic phase behavior and organization of dipalmitoylphosphatidylcholine bilayer membranes. *Biophys. J.* 91, 3327–3340.
- (48) Jain, M. K., and Berg, O. G. (2006) Coupling of the i-face and the active site of phospholipase A2 for interfacial activation. *Curr. Opin. Chem. Biol.* 10, 473–479.
- (49) Wong-Ekkabut, J., Xu, Z., Triampo, W., Tang, I. M., Tieleman, D. P., and Monticelli, L. (2007) Effect of lipid peroxidation on the properties of lipid bilayers: a molecular dynamics study. *Biophys. J.* 93, 4225–4236.
- (50) Bruch, R. C., and Thayer, W. S. (1983) Differential effect of lipid peroxidation on membrane fluidity as determined by electron spin resonance probes. *Biochim. Biophys. Acta* 733, 216–222.
- (51) McKinney, M. K., and Cravatt, B. F. (2005) Structure and function of fatty acid amide hydrolase. *Annu. Rev. Biochem.* 74, 411–432.
- (52) Fezza, F., De Simone, C., Amadio, D., and Maccarrone, M. (2008) Fatty acid amide hydrolase: a gate-keeper of the endocannabinoid system. *Subcell. Biochem.* 49, 101–132.
- (53) Tiburu, E. K., Tyukhtenko, S., Zhou, H., Janero, D. R., Struppe, J., and Makriyannis, A. (2011) Human cannabinoid 1 GPCR C-terminal domain interacts with bilayer phospholipids to modulate the structure of its membrane environment. *AAPS J.* 13, 92–98.
- (54) Rapaport, D., and Shai, Y. (1991) Interaction of fluorescently labeled pardaxin and its analogues with lipid bilayers. *J. Biol. Chem.* 266, 23769–23775.
- (55) Parasassi, T., De Stasio, G., d'Ubaldo, A., and Gratton, E. (1990) Phase fluctuation in phospholipid membranes revealed by Laurdan fluorescence. *Biophys. J.* 57, 1179–1186.